

---

# Self-Adaptive Training: beyond Empirical Risk Minimization

---

Lang Huang<sup>1</sup> Chao Zhang<sup>1</sup> Hongyang Zhang<sup>2</sup>

## Abstract

We propose self-adaptive training—a new training algorithm that dynamically corrects problematic training labels by model predictions without incurring extra computational cost—to improve generalization of deep learning for potentially corrupted training data. This problem is crucial towards robustly learning from data that are corrupted by, e.g., label noises and out-of-distribution samples. The standard empirical risk minimization (ERM) for such data, however, may easily overfit noises and thus suffers from sub-optimal performance. In this paper, we observe that model predictions can substantially benefit the training process: self-adaptive training significantly improves generalization over ERM under various levels of noises, and mitigates the overfitting issue in both natural and adversarial training. We evaluate the error-capacity curve of self-adaptive training: the test error is monotonously decreasing w.r.t. model capacity. This is in sharp contrast to the recently-discovered double-descent phenomenon in ERM which might be a result of overfitting of noises. Experiments on CIFAR and ImageNet datasets verify the effectiveness of our approach in two applications: classification with label noise and selective classification. We release our code at <https://github.com/LayneH/self-adaptive-training>.

## 1. Introduction

Due to impressive generalization performance, empirical risk minimization (ERM) has attracted tremendous attention in many fields, such as image classification (Simonyan & Zisserman, 2014; He et al., 2016). However, recent works (Zhang et al., 2016; Nagarajan & Kolter, 2019) cast doubt on the traditional views on ERM: techniques such as uniform convergence might be unable to explain the generalization of deep neural networks, because the ERM easily

overfits training data even though the training data are partially or completely corrupted by random noises.

Regarding this phenomenon, we conduct experiments on the CIFAR10 dataset (Krizhevsky & Hinton, 2009) with 40% of data being corrupted at random (see Section 2 for the detailed setting). Figure 1a displays the accuracy curves of ERM that are trained on the noisy training sets. It shows that, on all four corrupted datasets, the models easily overfit noisy training data and achieve nearly perfect training accuracy. However, these models exhibit substantially different generalization behaviors which are indistinguishable by the training accuracy.

Despite a large literature devoted to analyzing this phenomenon either in the theoretical or empirical manners, many fundamental questions remain unresolved. To name a few, Zhang et al. (2016) showed that early stopping can improve generalization. On the theoretical front, the work of (Li et al., 2019) considered the case where the labels are noisy, and proved that the first few training iterations fits the correct labels and overfitting only occurs in the last few iterations. For a concrete example, in Figure 1a, the accuracy increases in the early stage and the generalization errors grow quickly after certain epochs. Admittedly, stopping at early epoch improves generalization in the presence of label noises (see the first column in Figure 1a); however, it remains unclear how to properly choose such an epoch. Moreover, the early-stop mechanism may hurt performance on the validation sets in the other three corruption setups (see the other three columns in Figure 1a).

Our work is motivated by the above-mentioned observations and goes beyond the ERM. We begin by making the following observation in Figure 1a: the peak of accuracy curve on the clean data is much higher than the percentage of clean data in the noisy training set. This finding was also previously reported by Rolnick et al. (2017); Guan et al. (2018); Li et al. (2019) under label corruption setting and suggested that model predictions might be able to magnify useful underlying information in data. We confirm this finding and show that the pattern occurs broadly under various kinds of corruptions as well (see Figure 1a). Inspired by the observations, we propose *self-adaptive training*, a carefully designed approach which dynamically uses model predictions as a guiding principle in the design of training

<sup>1</sup>Peking University <sup>2</sup>Toyota Technological Institute at Chicago. Correspondence to: Chao Zhang <c.zhang@pku.edu.cn>, Hongyang Zhang <hongyanz@ttic.edu>.

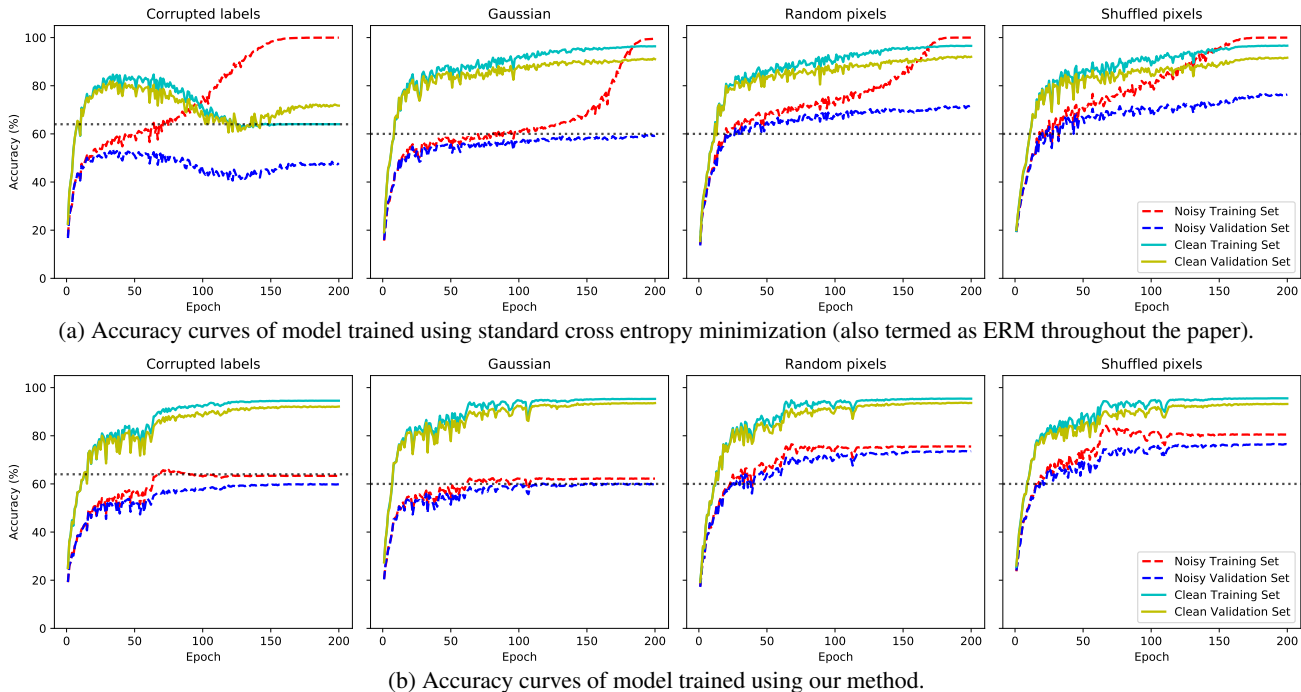


Figure 1: Accuracy curves of model trained on noisy CIFAR10 training set (corresponding to the red dashed curve). We construct the noisy sets by corrupting data with: (1) assign labels uniformly at random; (2) replace images by random Gaussian noises; (3) shuffle the pixels of images independently; (4) shuffle the pixels of images using the same chosen permutation. The horizontal dotted line displays the percentage of clean data in the training sets. It shows that while standard cross entropy training suffers from overfitting of noises, our method enjoys improved generalization and higher validation accuracy (e.g., the improvement is as large as 10% in the most left column).

algorithm. Figure 1b shows that our approach significantly alleviates the overfitting issue on noisy training data, reduces the generalization error on the corrupted distributions, and improves the performance on the clean distribution.

### 1.1. Summary of our contributions

Our work sheds light on understanding generalization of deep neural networks in an empirical manner.

- We analyze the standard ERM training process of deep networks on four kinds of potentially corrupted training data (see Figure 1a). We describe the characteristic failure patterns of ERM and observe that model predictions magnify useful underlying information in data. The observation motivates us to propose self-adaptive training, a new training algorithm which dynamically corrects problematic training labels by model predictions. Our approach significantly outperforms the standard cross entropy training under various noise rates (see Figures 1 and 2), without requiring modification to existing network architecture and incurring extra computational cost.
- We evaluate the error-capacity curve of self-adaptive training: the test error is monotonously decreasing w.r.t.

model capacity (see Figure 3). This is in sharp contrast to the recently-discovered double-descent phenomenon in ERM which might be a result of overfitting of noises.

- We inspect the adversarial robustness of self-adaptive training. We find that state-of-the-art adversarial training algorithm overfits adversarial examples. Our approach mitigates the overfitting issue and improves adversarial robustness (see Figure 4).

Self-adaptive training has two significant applications and advances the state-of-the-art in multiple ways.

- Classification with label noise, where the goal is to improve performance of deep networks on the clean test data in the presence of label noises in the training data. On manually corrupted CIFAR datasets, our approach consistently achieves  $\sim 2\%$  absolute improvement over previous best performed methods under varying noise rates. In the standard setup of training models on the ImageNet dataset, our approach improves ERM baseline by  $\sim 0.5\%$  in absolute.
- Selective classification, which aims to trade prediction coverage off against classification accuracy. Our approach can achieve up to 50% relative improvement under varying coverage rates on two datasets.

## 2. Generalization of Deep Networks

### 2.1. Corrupted data

We start this section by analyzing the standard training process of deep neural networks on four kinds of corrupted training data (Zhang et al., 2016). The experiments are conducted on the CIFAR10 dataset (Krizhevsky & Hinton, 2009), of which we split the original training data into a training set (consists of first 45,000 data pairs) and a validation set (consists of last 5,000 data pairs). We use data augmentation (e.g., random cropping and flip) and weight decay in our experiments if not specified. The rest experimental settings are the same as Section 3.2.

For randomization scheme, we consider the following cases where the data are *partially* corrupted with probability  $p$ : (1) **Corrupted labels**. Labels are assigned uniformly at random; (2) **Gaussian**. Images are replaced by random Gaussian samples with the same mean and standard deviation as the original image distribution; (3) **Random pixels**. Pixels of each image are shuffled using independently random permutations; (4) **Shuffled pixels**. Pixels of each image are shuffled using a fixed permutation pattern.

**Baseline results** In (Zhang et al., 2016), the authors showed that the model trained by standard cross entropy minimization can easily fit randomized data. However, they only reported the generalization errors under varying rates of label corruptions. Here, we report the whole training process and also consider the performance on clean sets (i.e., the original uncorrupted data). Figure 1a shows the four accuracy curves (on clean and noisy training, validation set, respectively) for each model that is trained on one of four corrupted training data. Note that the models can only have access to the noisy training sets (i.e., the red curve) and the other three curves are shown for the illustration purpose. We conclude two principal observations from the figures:

1. The accuracies on noisy training and validation sets are close at beginning and the gap is increasing w.r.t. epoch. The generalization errors (i.e., the gap between the accuracies on noisy training and validation sets) are large at the end of training.
2. The accuracy on clean training and validation set is consistently higher than the percentage of clean data in the noisy training set, around the epochs between underfitting and overfitting.

The first observation characterizes the typical failure patterns of prevailing training dynamic and conforms with the claims of previous work (Li et al., 2019). This poses concerns on the standard training dynamic of cross entropy minimization. The work of (Li et al., 2019) only considered the case of corrupted labels and proposed using early-stop

---

### Algorithm 1 Self-Adaptive Training

---

**Input:** Data  $\{(\mathbf{x}_i, \mathbf{y}_i)\}_n$ , total epochs  $E$ , batch size  $m$ , classifier  $f$ , initial epochs  $E_s = 60$ , momentum  $\alpha = 0.9$   
**Output:** Well generalized classifier  $f$   
 Initialize  $\{\mathbf{t}_i\}_n = \{\mathbf{y}_i\}_n$   
**for**  $e = 1$  **to**  $E$  **do**  
   **repeat**  
     Fetch mini-batch data  $\{(\mathbf{x}_i, \mathbf{t}_i)\}_m$   
     **for**  $i = 1$  **to**  $m$  **do**  
        $\mathbf{p}_i = \text{softmax}(f(\mathbf{x}_i))$   
       **if**  $e > E_s$  **then**  
          $\mathbf{t}_i = \alpha \times \mathbf{t}_i + (1 - \alpha) \times \mathbf{p}_i$   
       **end if**  
        $w_i = \max_j \mathbf{t}_{i,j}$   
     **end for**  
      $\mathcal{L}(f) = -\frac{1}{\sum_i w_i} \sum_i w_i \sum_j \mathbf{t}_{i,j} \log \mathbf{p}_{i,j}$   
     Update  $f$  by SGD on  $\mathcal{L}(f)$   
**until** epoch finished  
**end for**

---

mechanism to improve the performance on clean data. However, our analysis on the broader range of corruptions shows that the early stopping might be sub-optimal and may hurt the performance under other types of corruptions (see the last three columns in Figure 1a).

The second observation implies that, perhaps surprisingly, deep network can capture and magnify useful signals in the noisy training set, although the training dataset is heavily corrupted. This was also reported in (Zhang et al., 2016; Rolnick et al., 2017; Guan et al., 2018; Li et al., 2019), and we confirm its common occurrence under various kinds of corruptions. This observation is of essence to improve the generalization of deep networks and sheds light on our approach: to incorporate model predictions into training procedure.

### 2.2. Our approach: Self-Adaptive Training

**Notations** We consider  $c$ -class classification problem and denote the images by  $\mathbf{x}_i \in \mathbb{R}^d$ , labels by  $\mathbf{y}_i \in \{0, 1\}^c$ ,  $\mathbf{y}_i^\top \mathbf{1} = 1$ . The images  $\mathbf{x}_i$  or labels  $\mathbf{y}_i$  might be corrupted by one of four randomization schemes we have previously described. We denote the logits of the classifier (e.g., parameterized by a deep neural network) by  $f(\cdot)$ .

**The blessing of model predictions** How to properly incorporate model predictions is of core importance in our approach. A straight-forward scheme is to use a convex combination of labels and predictions as our training targets. Concretely, given data pair  $(\mathbf{x}_i, \mathbf{y}_i)$  and prediction  $\mathbf{p}_i = \text{softmax}(f(\mathbf{x}_i))$ , we use training target  $\mathbf{t}_i = \alpha \times \mathbf{y}_i + (1 - \alpha) \times \mathbf{p}_i$ . Then, cross entropy loss between  $\mathbf{p}_i$  and  $\mathbf{t}_i$  is minimized to update the classifier  $f$  in each

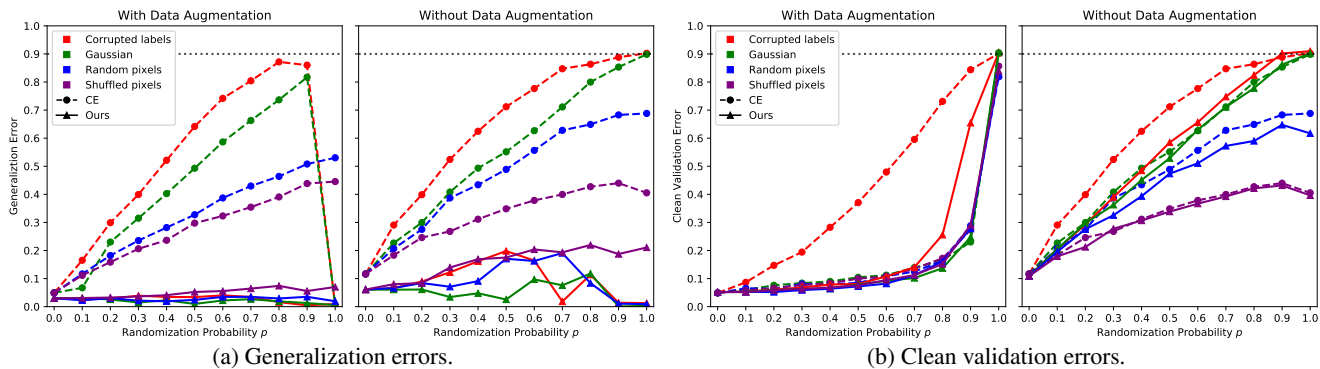


Figure 2: Generalization and clean validation errors under four randomization schemes (represented by different colors) for standard cross entropy (dashed curves) and our approach (solid curves) on CIFAR10. We conduct experiments where models are trained with or without data augmentation (i.e., random cropping and flipping). It shows that self-adaptive training has superior performance with and without data corruptions.

training iteration.

This naive scheme suffers from multiple drawbacks: (1) model predictions are inaccurate in the early stage of training and may be unstable due to some explicit regularization techniques (e.g., data augmentation and dropout (Srivastava et al., 2014)). This leads to instability of  $t_i$ ; (2) this scheme can assign at most  $1 - \alpha$  weight on the true class when  $y_i$  is corrupted. However, we aim to correct the erroneous labeling (i.e., assign nearly 100% weight on the true class).

Here, we propose using accumulated predictions to augment the training dynamic. Formally, we initialize  $t_i \leftarrow y_i$ , fix  $t_i$  in the first  $E_s$  training epochs, and update

$$t_i \leftarrow \alpha \times t_i + (1 - \alpha) \times p_i \quad (1)$$

in each following training epoch. The exponential-moving-average scheme alleviates the instability of model predictions and smooths  $t_i$  during the training process. This also enables our algorithm to completely change the training labels if necessary. Momentum term  $\alpha$  controls the weight of using model predictions. The number of initial epochs  $E_s$  allows the model to capture informative signals in data and excludes ambiguous information that is provided by model predictions in the early stage of training.

**Sample re-weighting** Building upon the scheme presented above, we introduce a simple yet effective sample re-weighting scheme based on the maximal prediction on each sample. Concretely, given training target  $t_i$ , we set

$$w_i = \max_j t_{i,j}. \quad (2)$$

Sample weight  $w_i \in [\frac{1}{c}, 1]$  reveals the labeling confidence of this sample. Intuitively, all samples are treated equally in the first  $E_s$  epochs. As target  $t_i$  being updated, our algorithm pays less attention to potentially erroneous data and learns more on likely uncorrupted data. This re-weighting scheme also allows the corrupted samples to re-attain attention if they are confidently corrected.

**Putting everything together** We use stochastic gradient descent to minimize:

$$\mathcal{L}(f) = -\frac{1}{\sum_i w_i} \sum_i w_i \sum_j t_{i,j} \log p_{i,j} \quad (3)$$

during the training process. Here, the denominator normalizes per sample weights and stabilizes the loss scale.

We name our approach *Self-Adaptive Training* and display the pseudocode in Algorithm 1. We fix the introduced hyperparameters  $E_s = 60$ ,  $\alpha = 0.9$  in all following experiments if not specified for convenience. Our approach can be viewed as a drop-in replacement of standard cross entropy training, requiring no modification to existing network architecture and incurring almost no extra computational cost.

### 2.3. Improved generalization

We repeat the same experiments in Section 2.1 by replacing the standard cross entropy minimization with our approach. Detailed experiment settings are given in Section 3.2. In Figure 1b, we plot the accuracy curves of models trained with our approach on four corrupted training set to compare with those in Figure 1a. We highlight several significant improvements over the baselines.

First, self-adaptive training mitigates the overfitting issue in deep networks. The accuracy curves on noisy training set (i.e., the red dashed curves in Figure 1b) eventually converge to values that slightly higher than the percentage of clean data in the training sets, and do not reach perfect accuracy.

Second, our approach improves generalization of deep networks. We observe that the generalization errors of self-adaptive training (the gap between red and blue dashed curves in Figure 1b) are much smaller than those of baselines. We further confirm this observation by displaying the generalization errors of the models trained on all four corrupted training sets under various noise rates in the left



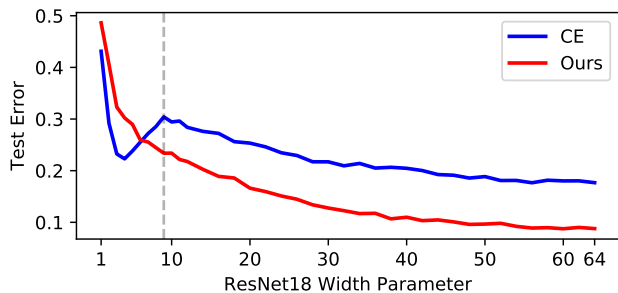


Figure 3: Self-adaptive training vs. ERM on the error-capacity curve. We train the networks on the CIFAR10 dataset with 15% randomly-corrupted labels and report the test errors on the clean data. The model of width 64 corresponds to the standard ResNet-18. The vertical dashed line represents the interpolation threshold. It shows that self-adaptive training has vanished double-descent phenomenon.

subfigure of Figure 2a. Generalization errors of standard cross entropy based training algorithms consistently grow as we increase the injected noise level, except for the cases of 100% label and Gaussian noises where the model fits completely the noises. In contrast, our approach reduces the generalization errors to substantial lower values, even though we vary the noise levels from 0% (no noise) to 100% (complete noise).

Last, our approach improves the performance on the clean datasets. The accuracy on the clean sets (cyan and yellow solid curves in Figure 1b) consistently increases and converges to higher values than the baselines. We display detailed comparisons of the clean validation errors in the left of Figure 2b. The figure depicts the significant slow-down of the error growth and the consistent improvements when equipped with our approach. This finding indicates that our approach does not trivially underfit noisy training data but indeed calibrates training process and improves generalization of deep networks.

**Effect of data augmentation** All our previous studies are performed with common data augmentation (i.e., random cropping and flipping). Here, we further report the effect of data augmentation. We adjust introduced hyper-parameters as  $E_s = 25$ ,  $\alpha = 0.7$  due to severer overfitting when data augmentation is absent. The right subfigures of Figure 2a and 2b show the corresponding generalization errors and clean validation errors. We observe that, for both standard cross entropy and our approach, the errors clearly increase when data augmentation is absent. However, the gain is limited and the generalization errors can still be very large, with or without data augmentation for standard cross entropy minimization. Directly replacing standard training procedure with our approach can bring bigger gains in terms of generalization regardless of data augmentation. This suggests that data augmentation can help but is not of essence to improve generalization of deep neural networks, which is

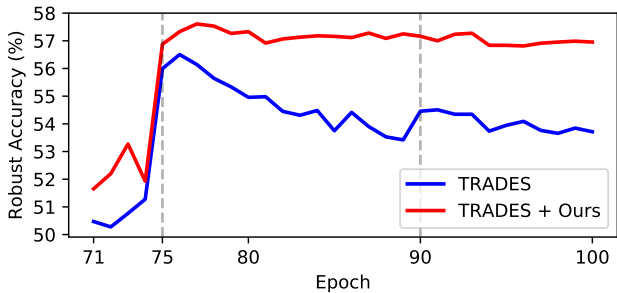


Figure 4: Robust Accuracy (%) on CIFAR10 test set under white box  $\ell_\infty$  PGD-20 attack ( $\epsilon = 0.031$ ). The vertical dashed lines indicate learning rate decay. It shows that self-adaptive training consistently improves TRADES.

consistent with the observation in (Zhang et al., 2016).

#### 2.4. Vanished double-descent phenomenon

A line of works (Oppor, 1995; 2001; Advani & Saxe, 2017; Spigler et al., 2018; Belkin et al., 2018; Geiger et al., 2019; Nakkiran et al., 2019) observe an intriguing phenomenon in modern machine learning models: as the capacity of model increases, the test error initially decreases, then increases, and finally shows a second descent. This phenomenon is termed *double descent* by Belkin et al. (2018) and commonly occurs in deep networks (Nakkiran et al., 2019).

We follow exactly the same experimental settings as in (Nakkiran et al., 2019) to reproduce this phenomenon: we vary the width parameter of ResNet-18 (He et al., 2016) and train the networks on CIFAR10 dataset with 15% training label being corrupted at random (details are given in Appendix A.1). Figure 3 depicts the curves of test error. We observe that the curve of cross entropy minimization exhibits the double-descent phenomenon, while the curve of our approach is monotonously decreasing as the model capacity increases. Notably, Nakkiran et al. (2019) reported that double-descent phenomenon is somewhat tricky to be reproduced and is diminished when label noise is absent. Our experiment indicates that the double-descent phenomenon may be a result of overfitting of noises and the proposed self-adaptive training can bypass this phenomenon.

#### 2.5. Mitigating overfitting in adversarial training

We evaluate the ability of self-adaptive training to improve model robustness to adversarial examples (Szegedy et al., 2013). The state-of-the-art adversarial training algorithm TRADES (Zhang et al., 2019) is used as our baseline. TRADES proposed to minimize:

$$\mathbb{E}_{\mathbf{x}, \mathbf{y}} \left\{ \text{CE}(\mathbf{p}(\mathbf{x}), \mathbf{y}) + \max_{\|\tilde{\mathbf{x}} - \mathbf{x}\|_\infty \leq \epsilon} \text{KL}(\mathbf{p}(\mathbf{x}), \mathbf{p}(\tilde{\mathbf{x}})) / \lambda \right\}, \quad (4)$$

Table 1: Test Accuracy (%) on CIFAR10 and CIFAR100 datasets with various levels of uniform label noise injected to training set. We compare with previous works under exactly the same experiment settings. The best entries are bold faced.

METHOD	CIFAR10				CIFAR100			
	LABEL NOISE RATE				LABEL NOISE RATE			
	0.2	0.4	0.6	0.8	0.2	0.4	0.6	0.8
CE + EARLY STOPPING	85.57	81.82	76.43	60.99	63.70	48.60	37.86	17.28
LABEL SMOOTHING (SZEGEDY ET AL., 2016)	85.64	71.59	50.51	28.19	67.44	53.84	33.01	9.74
FORWARD $\hat{T}$ (PATRINI ET AL., 2017)	87.99	83.25	74.96	54.64	39.19	31.05	19.12	8.99
MIXUP (ZHANG ET AL., 2017)	93.58	89.46	78.32	66.32	69.31	58.12	41.10	18.77
TRUNC $\mathcal{L}_q$ (ZHANG & SABUNCU, 2018)	89.70	87.62	82.70	67.92	67.61	62.64	54.04	29.60
JOINT OPT (TANAKA ET AL., 2018)	92.25	90.79	86.87	69.16	58.15	54.81	47.94	17.18
SCE (WANG ET AL., 2019)	90.15	86.74	80.80	46.28	71.26	66.41	57.43	26.41
DAC (THULASIDASAN ET AL., 2019)	92.91	90.71	86.30	74.84	73.55	66.92	57.17	32.16
SELF (NGUYEN ET AL., 2019)	-	91.13	-	63.59	-	66.71	-	35.56
OURS	<b>94.14</b>	<b>92.64</b>	<b>89.23</b>	<b>78.58</b>	<b>75.77</b>	<b>71.38</b>	<b>62.69</b>	<b>38.72</b>

Table 2: Top1 Accuracy (%) on ImageNet validation set.

METHOD	RESNET-50	RESNET-101
ERM	76.8	78.2
OURS	<b>77.2</b>	<b>78.7</b>

where  $p(\cdot)$  is the model prediction,  $\epsilon$  is the maximal allowed perturbation, CE stands for the cross entropy, KL stands for the Kullback-Leibler divergence, and the hyper-parameter  $\lambda$  controls the trade-off between these two terms. We directly replace the CE term in TRADES loss with our method in the experiments. The models are evaluated using robust accuracy  $\frac{1}{n} \sum_i \mathbb{1}\{\arg\max p(\tilde{x}_i) = \arg\max y_i\}$ , where adversarial example  $\tilde{x}$  are generated by white box  $\ell_\infty$  projected gradient descent (PGD) attack (Madry et al., 2017) with  $\epsilon = 0.031$ , perturbation steps of 20. We set the initial learning rate as 0.1 and decay it by a factor of 0.1 in epochs 75 and 90, respectively. We choose  $1/\lambda = 6.0$  as suggested by Zhang et al. (2019) and use  $E_s = 70$ ,  $\alpha = 0.9$  for our approach. Experimental details are given in Appendix A.2.

We display the robust accuracy on CIFAR10 test set after  $E_s = 70$  epochs in Figure 4. We can see that the robust accuracy of TRADES reaches its highest value around the epoch of first learning rate decay (epoch 75) and decreases later, which suggests that overfitting might happen if we train the model without early stopping. On the other hand, our method considerably mitigates the overfitting issue in the adversarial training and consistently improves the robust accuracy of TRADES by 1%~3% in absolute.

### 3. Classification with Label Noise

#### 3.1. Problem formulation

This task is similar to the corrupted label scheme that we considered in Section 2. Given a set of noisy training data  $\{(x_i, \tilde{y}_i)\}_n \in \tilde{\mathcal{D}}$ , where  $\tilde{\mathcal{D}}$  is the distribution of noisy data and  $\tilde{y}_i$  is the noisy label for each uncorrupted sample  $x_i$ ,

Table 3: Ablation study on influence of two components of our approach. We report classification Accuracy (%) on CIFAR datasets under uniform label noise.

NOISE RATE	CIFAR10		CIFAR100	
	0.4	0.8	0.4	0.8
OURS	<b>92.64</b>	<b>78.58</b>	<b>71.38</b>	<b>38.72</b>
- RE-WEIGHTING	92.49	78.10	69.52	36.78
- MOVING AVERAGE	72.00	28.17	50.93	11.57

the goal is to be robust to the massive label noises in the training data and improve the classification performance on clean test data that are sampled from clean distribution  $\mathcal{D}$ .

#### 3.2. Experiments on manually corrupted datasets

**Setup** We consider the case that various amount of uniform label noises (i.e., labels are assigned uniformly at random) are injected. Following (Zhang & Sabuncu, 2018; Thulasidasan et al., 2019), we conduct experiments on CIFAR10 and CIFAR100 datasets (Krizhevsky & Hinton, 2009) and use ResNet-34 (He et al., 2016) as base classifier. The networks are implemented on PyTorch (Paszke et al., 2019) and optimized using SGD with initial learning rate of 0.1, momentum of 0.9, weight decay of 0.0005, batch size of 256, total training epochs of 200. The learning rate is decayed using cosine annealing schedule (Loshchilov & Hutter, 2016) to 0. The random horizontal flipping and cropping augmentation is turned on. For our approach, we use default hyper-parameters  $\alpha = 0.9$ ,  $E_s = 60$  in all experiments. We report the average performance over 3 trials.

**Main results** We compare our approach with the state-of-the-art and summarize the results in Table 1. Most of the results are cited from original papers when they are under the same experiment settings, except that the results of Label Smoothing (Szegedy et al., 2016), Mixup (Zhang et al., 2017), Joint Opt (Tanaka et al., 2018) and SCE (Wang et al., 2019) are reproduced based on official open-sourced implementations. From the table, we can see that our ap-

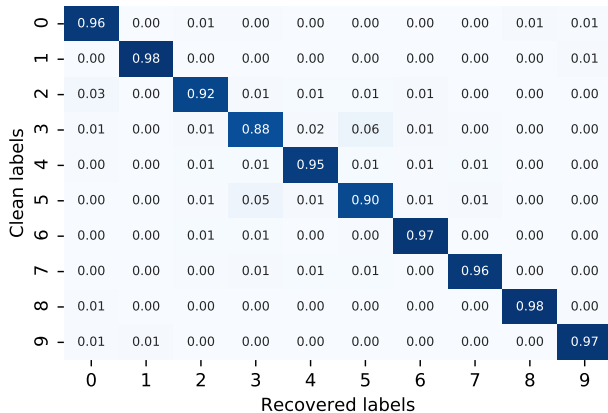


Figure 5: Confusion matrix of recovered labels w.r.t clean labels on CIFAR10 training set when 40% of training labels are assigned u.a.r.. The overall recovery accuracy is 94.65%.

proach outperforms the state-of-the-art methods in most entries by 1% ~ 5% on both CIFAR10 and CIFAR100 datasets. Notably, unlike Joint Opt, DAC and SELF methods that require multiple iterations of training, our method is straight-forward and enjoys the same computational budget as the standard training.

**Ablation study** First, we report the performance of standard cross entropy minimization equipped with simple early stopping scheme in the first row of Table 1. We observe that our approach achieves substantial improvements over this baseline. This demonstrates that simple early stopping scheme is a sub-optimal solution and shows the advantages of involving model predictions in the training process. Then, we further report the influences of two individual components of our approach: exponential moving average and sample re-weighting scheme. As displayed in Table 3, removing any component considerably hurts the performance under all noise rates and removing exponential moving average scheme leads to a significant drop. This suggests that properly incorporating model predictions is of essence in our approach.

**Label recovery** We demonstrate that our approach is able to recover underlying true labels from noisy training labels. We directly obtain recovered labels according to moving average targets  $\mathbf{t}_i$  and compute the recovery accuracy as  $\frac{1}{n} \sum_i \mathbb{1}\{\arg\max \mathbf{y}_i = \arg\max \mathbf{t}_i\}$ , where  $\mathbf{y}_i$  is the clean label of each training sample. In Figure 5, we display the confusion matrix of recovered labels w.r.t the clean labels, where label noise of 40% is injected to the CIFAR10 training set and the percentage of remaining clean labels is  $\sim 64\%$ . Our approach successfully corrects a huge amount of labels for all classes and obtains a recovery accuracy of 94.65%.

### 3.3. Experiments on real-world noisy dataset

Russakovsky et al. (2015) suggested that ImageNet dataset

(Deng et al., 2009) contains annotation errors even after several rounds of cleaning. In this section, we use ResNets (He et al., 2016) to evaluate self-adaptive training on this real-world noisy dataset. Experimental details are given in Appendix A.3. Note that we do not inject any extra noise into this dataset but use original labels in the experiments.

We report model performance on the ImageNet validation set in terms of top1 accuracy in Table 2. From the results, we can see that self-adaptive training consistently improves the standard ERM baseline by 0.4% ~ 0.5%, which validates the effectiveness of our approach on real-world noisy dataset.

## 4. Selective Classification

### 4.1. Problem formulation

Selective classification, a.k.a. classification with rejection, trades classifier coverage off against accuracy (El-Yaniv & Wiener, 2010), where the coverage is defined as the ratio of the number of classified samples to the total size of original dataset. The task focuses on noise-free setting and allows classifier to abstain on potential out-of-distribution samples or samples lies in the tail of data distribution, that is, making prediction only on samples with confidence. Formally, a selective classifier is a composition of two functions  $(f, g)$ , where  $f$  is the conventional  $c$ -class classifier and  $g$  is the selection function that reveals the underlying uncertainty of inputs. Given an input  $\mathbf{x}$ , selective classifier outputs

$$(f, g)(\mathbf{x}) = \begin{cases} \text{Abstain}, & g(\mathbf{x}) > \tau; \\ f(\mathbf{x}), & \text{otherwise}, \end{cases} \quad (5)$$

for a given threshold  $\tau$  that controls the trade-off.

### 4.2. Approach

Inspired by (Thulasidasan et al., 2019; Liu et al., 2019), we adapt our presented approach in Algorithm 1 to the selective classification task. We introduce an extra  $(c + 1)$ -th class (represents *abstention*) during training and replace selection function  $g(\cdot)$  in Equation (5) by  $f(\cdot)_c$ . In this way, we can train a selective classifier in an end-to-end fashion. Besides, unlike previous works that provide no explicit signal for learning abstention class, we propose using model predictions as a guideline in the design of learning process.

Given a mini-batch of data pairs  $\{(\mathbf{x}_i, \mathbf{y}_i)\}_m$ , model predictions  $\mathbf{p}_i$  and its exponential moving average  $\mathbf{t}_i$  for each sample, we optimize the classifier  $f$  by minimizing:

$$\mathcal{L}(f) = -\frac{1}{m} \sum_i [\mathbf{t}_{i, y_i} \log \mathbf{p}_{i, y_i} + (1 - \mathbf{t}_{i, y_i}) \log \mathbf{p}_{i, c}], \quad (6)$$

where  $y_i$  represents the non-zero index of  $\mathbf{y}_i$ . The first term

Table 4: Selective classification error rate (%) on CIFAR10 and Dogs vs. Cats datasets for various coverage rates (%). Mean and standard deviation are calculated over 3 trials. The best entries and those overlap with them are marked bold.

DATASET	COVERAGE	METHOD				
		OURS	DEEP GAMBLERS	SELECTIVENET	SR	MC-DROPOUT
CIFAR10	100	6.05±0.20	6.12±0.09	6.79±0.03	6.79±0.03	6.79±0.03
	95	<b>3.37±0.05</b>	<b>3.49±0.15</b>	4.16±0.09	4.55±0.07	4.58±0.05
	90	<b>1.93±0.09</b>	2.19±0.12	2.43±0.08	2.89±0.03	2.92±0.01
	85	<b>1.15±0.18</b>	<b>1.09±0.15</b>	1.43±0.08	1.78±0.09	1.82±0.09
	80	<b>0.67±0.10</b>	<b>0.66±0.11</b>	0.86±0.06	1.05±0.07	1.08±0.05
	75	<b>0.44±0.03</b>	0.52±0.03	<b>0.48±0.02</b>	0.63±0.04	0.66±0.05
	70	<b>0.34±0.06</b>	0.43±0.07	<b>0.32±0.01</b>	0.42±0.06	0.43±0.05
DOGS VS. CATS	100	3.01±0.17	2.93±0.17	3.58±0.04	3.58±0.04	3.58±0.04
	95	<b>1.25±0.05</b>	<b>1.23±0.12</b>	1.62±0.05	1.91±0.08	1.92±0.06
	90	<b>0.59±0.04</b>	<b>0.59±0.13</b>	0.93±0.01	1.10±0.08	1.10±0.05
	85	<b>0.25±0.11</b>	0.47±0.10	0.56±0.02	0.82±0.06	0.78±0.06
	80	<b>0.15±0.06</b>	0.46±0.08	0.35±0.09	0.68±0.05	0.55±0.02

measures the cross-entropy loss between prediction and original label  $y_i$ , in order to learn a good multi-class classifier. The second term acts as the selection function, identifies uncertain samples in datasets. The moving average  $t_{i,y_i}$  dynamically trades-off these two terms: if  $t_{i,y_i}$  is very small, the sample is deemed as uncertain and the second term enforces the selective classifier to learn to abstain this sample; if  $t_{i,y_i}$  is close to 1, the loss recovers the standard cross entropy minimization and enforces the selective classifier to make perfect prediction.

### 4.3. Experiments

We perform experiments on two datasets: CIFAR10 (Krizhevsky & Hinton, 2009) and Dogs vs. Cats (cat). We compare our method with previous state-of-the-art methods on selective classification, including Deep Gamblers (Liu et al., 2019), SelectiveNet (Geifman & El-Yaniv, 2019), Softmax Response (SR) and MC-dropout (Geifman & El-Yaniv, 2017). We use the same experimental settings as these works to ensure fair comparison (details are given in Appendix A.4). The results of these methods are directly cited from original papers and summarized in Table 4. We see that our method achieves up to 50% relative improvements compared with all other methods under various coverage rates, on all datasets. Notably, Deep Gamblers also introduces an extra abstention class in their method but without applying model predictions. The superior performance of our method indicates the importance of incorporating model predictions into learning.

## 5. Related Works

Previous work (Zhang et al., 2016) systematically analyzed the capability of deep networks to overfit random noise. Their results show that traditional wisdom fails to explain the generalization of deep networks. Another line of works (Oppen, 1995; 2001; Advani & Saxe, 2017; Spigler

et al., 2018; Belkin et al., 2018; Geiger et al., 2019; Nakkiran et al., 2019) observed an double-descent risk curve from the bias-variance trade-off. Belkin et al. (2018); Nakkiran et al. (2019) claimed that this observation challenges the conventional U-shaped risk curve in the textbook. Our work shows that these intriguing observations may stem from overfitting of noises; the phenomenon vanishes by a proper design of training process such as the self-adaptive training.

There have been many works on learning from noisy data. Arpit et al. (2017); Li et al. (2019) showed that deep neural networks tend to fit clean samples first and overfitting of noise occurs in the later stage of training. Li et al. (2019) further proved that early stopping can mitigate the issues that are caused by label noises. We show that our approach achieves significant improvement. Tanaka et al. (2018); Bagherinezhad et al. (2018) used the first few rounds of training to update noisy training labels and the last round of training to train on the updated labels; Nguyen et al. (2019) used moving average of model predictions to filter out uncertainty in each round of training and fine-tuned the model on the de-noised data. In contrast, our approach is a drop-in replacement of standard cross entropy training and incurs almost no extra computational cost. Reed et al. (2014); Dong et al. (2019) incorporated model predictions into training by simple interpolation of labels and model predictions. We demonstrate that our exponential moving average and sample re-weighting schemes enjoy superior performance.

In terms of improving generalization of ERM, Szegedy et al. (2016); Pereyra et al. (2017) proposed label smoothing regularization that uniformly distributes  $\epsilon$  of labeling weight to all classes and uses this soft label for training; Zhang et al. (2017) introduced mixup augmentation that extends the training distribution by dynamic interpolations between random paired input images and the associated targets during training. These methods are similar with ours in that



using soft label for training. However, self-adaptive training is able to recover true labels from noisy labels and is more robust to underlying noises.

## 6. Conclusion

In this paper, we study the generalization of deep networks. We analyze the standard training dynamic using cross entropy and characterize its intrinsic failure patterns. Our observations motivate us to propose Self-Adaptive Training that incorporates model predictions into training process. We demonstrate that our approach improves the generalization of deep networks and casts doubt on recently-discovered double-descent phenomenon. Finally, we present two applications of self-adaptive training on classification with label noise and selective classification, where our approach significantly advances the state-of-the-art.

## References

- Dogs vs. cats dataset. <https://www.kaggle.com/c/dogs-vs-cats>.
- Advani, M. S. and Saxe, A. M. High-dimensional dynamics of generalization error in neural networks. *arXiv preprint arXiv:1710.03667*, 2017.
- Arpit, D., Jastrzbski, S., Ballas, N., Krueger, D., Bengio, E., Kanwal, M. S., Maharaj, T., Fischer, A., Courville, A., Bengio, Y., et al. A closer look at memorization in deep networks. In *Proceedings of the 34th International Conference on Machine Learning-Volume 70*, pp. 233–242. JMLR. org, 2017.
- Bagherinezhad, H., Horton, M., Rastegari, M., and Farhadi, A. Label refinery: Improving imagenet classification through label progression. *arXiv preprint arXiv:1805.02641*, 2018.
- Belkin, M., Hsu, D., Ma, S., and Mandal, S. Reconciling modern machine learning and the bias-variance trade-off. *arXiv preprint arXiv:1812.11118*, 2018.
- Deng, J., Dong, W., Socher, R., Li, L.-J., Li, K., and Fei-Fei, L. Imagenet: A large-scale hierarchical image database. In *Proceedings of the IEEE Conference on Computer Vision and Pattern Recognition*, pp. 248–255. Ieee, 2009.
- Dong, B., Hou, J., Lu, Y., and Zhang, Z. Distillation  $\approx$  early stopping? harvesting dark knowledge utilizing anisotropic information retrieval for overparameterized neural network. *arXiv preprint arXiv:1910.01255*, 2019.
- El-Yaniv, R. and Wiener, Y. On the foundations of noise-free selective classification. *Journal of Machine Learning Research*, 11(May):1605–1641, 2010.
- Geifman, Y. and El-Yaniv, R. Selective classification for deep neural networks. In *Advances in Neural Information Processing Systems*, pp. 4878–4887, 2017.
- Geifman, Y. and El-Yaniv, R. Selectivenet: A deep neural network with an integrated reject option. In *International Conference on Machine Learning*, pp. 2151–2159, 2019.
- Geiger, M., Spigler, S., d’Ascoli, S., Sagun, L., Baity-Jesi, M., Biroli, G., and Wyart, M. Jamming transition as a paradigm to understand the loss landscape of deep neural networks. *Physical Review E*, 100(1):012115, 2019.
- Goyal, P., Dollr, P., Girshick, R., Noordhuis, P., Wesolowski, L., Kyrola, A., Tulloch, A., Jia, Y., and He, K. Accurate, large minibatch sgd: Training imagenet in 1 hour. *arXiv preprint arXiv:1706.02677*, 2017.
- Guan, M. Y., Gulshan, V., Dai, A. M., and Hinton, G. E. Who said what: Modeling individual labelers improves classification. In *Thirty-Second AAAI Conference on Artificial Intelligence*, 2018.
- He, K., Zhang, X., Ren, S., and Sun, J. Deep residual learning for image recognition. In *Proceedings of the IEEE Conference on Computer Vision and Pattern Recognition*, pp. 770–778, 2016.
- Ioffe, S. and Szegedy, C. Batch normalization: Accelerating deep network training by reducing internal covariate shift. In *International Conference on Machine Learning*, pp. 448–456, 2015.
- Kingma, D. P. and Ba, J. Adam: A method for stochastic optimization. *arXiv preprint arXiv:1412.6980*, 2014.
- Krizhevsky, A. and Hinton, G. E. Learning multiple layers of features from tiny images. Technical report, University of Toronto, 2009.
- Li, M., Soltanolkotabi, M., and Oymak, S. Gradient descent with early stopping is provably robust to label noise for overparameterized neural networks. *arXiv preprint arXiv:1903.11680*, 2019.
- Liu, Z., Wang, Z., Liang, P. P., Salakhutdinov, R., Morency, L.-P., and Ueda, M. Deep gamblers: Learning to abstain with portfolio theory. In *Advances in Neural Information Processing Systems*, 2019.
- Loshchilov, I. and Hutter, F. Sgdr: Stochastic gradient descent with warm restarts. *arXiv preprint arXiv:1608.03983*, 2016.
- Madry, A., Makelov, A., Schmidt, L., Tsipras, D., and Vladu, A. Towards deep learning models resistant to adversarial attacks. *arXiv preprint arXiv:1706.06083*, 2017.

- Nagarajan, V. and Kolter, J. Z. Uniform convergence may be unable to explain generalization in deep learning. In *Advances in Neural Information Processing Systems*, pp. 11611–11622, 2019.
- Nakkiran, P., Kaplun, G., Bansal, Y., Yang, T., Barak, B., and Sutskever, I. Deep double descent: Where bigger models and more data hurt. *arXiv preprint arXiv:1912.02292*, 2019.
- Nguyen, D. T., Mummadi, C. K., Ngo, T. P. N., Nguyen, T. H. P., Beggel, L., and Brox, T. Self: Learning to filter noisy labels with self-ensembling. *arXiv preprint arXiv:1910.01842*, 2019.
- Opper, M. Statistical mechanics of learning: Generalization. *The Handbook of Brain Theory and Neural Networks*, pp. 922–925, 1995.
- Opper, M. Learning to generalize. *Frontiers of Life*, 3(part 2):763–775, 2001.
- Paszke, A., Gross, S., Massa, F., Lerer, A., Bradbury, J., Chanan, G., Killeen, T., Lin, Z., Gimelshein, N., Antiga, L., et al. Pytorch: An imperative style, high-performance deep learning library. In *Advances in Neural Information Processing Systems*, pp. 8024–8035, 2019.
- Patrini, G., Rozza, A., Krishna Menon, A., Nock, R., and Qu, L. Making deep neural networks robust to label noise: A loss correction approach. In *Proceedings of the IEEE Conference on Computer Vision and Pattern Recognition*, pp. 1944–1952, 2017.
- Pereyra, G., Tucker, G., Chorowski, J., Kaiser, Ł., and Hinton, G. Regularizing neural networks by penalizing confident output distributions. *arXiv preprint arXiv:1701.06548*, 2017.
- Reed, S., Lee, H., Anguelov, D., Szegedy, C., Erhan, D., and Rabinovich, A. Training deep neural networks on noisy labels with bootstrapping. *arXiv preprint arXiv:1412.6596*, 2014.
- Rolnick, D., Veit, A., Belongie, S., and Shavit, N. Deep learning is robust to massive label noise. *arXiv preprint arXiv:1705.10694*, 2017.
- Russakovsky, O., Deng, J., Su, H., Krause, J., Satheesh, S., Ma, S., Huang, Z., Karpathy, A., Khosla, A., Bernstein, M., et al. Imagenet large scale visual recognition challenge. *International Journal of Computer Vision*, 115(3): 211–252, 2015.
- Simonyan, K. and Zisserman, A. Very deep convolutional networks for large-scale image recognition. *arXiv preprint arXiv:1409.1556*, 2014.
- Spigler, S., Geiger, M., d’Ascoli, S., Sagun, L., Biroli, G., and Wyart, M. A jamming transition from under-to over-parametrization affects loss landscape and generalization. *arXiv preprint arXiv:1810.09665*, 2018.
- Srivastava, N., Hinton, G., Krizhevsky, A., Sutskever, I., and Salakhutdinov, R. Dropout: a simple way to prevent neural networks from overfitting. *The Journal of Machine Learning Research*, 15(1):1929–1958, 2014.
- Szegedy, C., Zaremba, W., Sutskever, I., Bruna, J., Erhan, D., Goodfellow, I., and Fergus, R. Intriguing properties of neural networks. *arXiv preprint arXiv:1312.6199*, 2013.
- Szegedy, C., Vanhoucke, V., Ioffe, S., Shlens, J., and Wojna, Z. Rethinking the inception architecture for computer vision. In *Proceedings of the IEEE Conference on Computer Vision and Pattern Recognition*, pp. 2818–2826, 2016.
- Tanaka, D., Ikami, D., Yamasaki, T., and Aizawa, K. Joint optimization framework for learning with noisy labels. In *Proceedings of the IEEE Conference on Computer Vision and Pattern Recognition*, pp. 5552–5560, 2018.
- Thulasidasan, S., Bhattacharya, T., Bilmes, J., Chennupati, G., and Mohd-Yusof, J. Combating label noise in deep learning using abstention. In *International Conference on Machine Learning*, pp. 6234–6243, 2019.
- Wang, Y., Ma, X., Chen, Z., Luo, Y., Yi, J., and Bailey, J. Symmetric cross entropy for robust learning with noisy labels. In *Proceedings of the IEEE International Conference on Computer Vision*, pp. 322–330, 2019.
- Zagoruyko, S. and Komodakis, N. Wide residual networks. *arXiv preprint arXiv:1605.07146*, 2016.
- Zhang, C., Bengio, S., Hardt, M., Recht, B., and Vinyals, O. Understanding deep learning requires rethinking generalization. *arXiv preprint arXiv:1611.03530*, 2016.
- Zhang, H., Cisse, M., Dauphin, Y. N., and Lopez-Paz, D. mixup: Beyond empirical risk minimization. *arXiv preprint arXiv:1710.09412*, 2017.
- Zhang, H., Yu, Y., Jiao, J., Xing, E., El Ghaoui, L., and Jordan, M. Theoretically principled trade-off between robustness and accuracy. In *International Conference on Machine Learning*, pp. 7472–7482, 2019.
- Zhang, Z. and Sabuncu, M. Generalized cross entropy loss for training deep neural networks with noisy labels. In *Advances in Neural Information Processing Systems*, pp. 8778–8788, 2018.

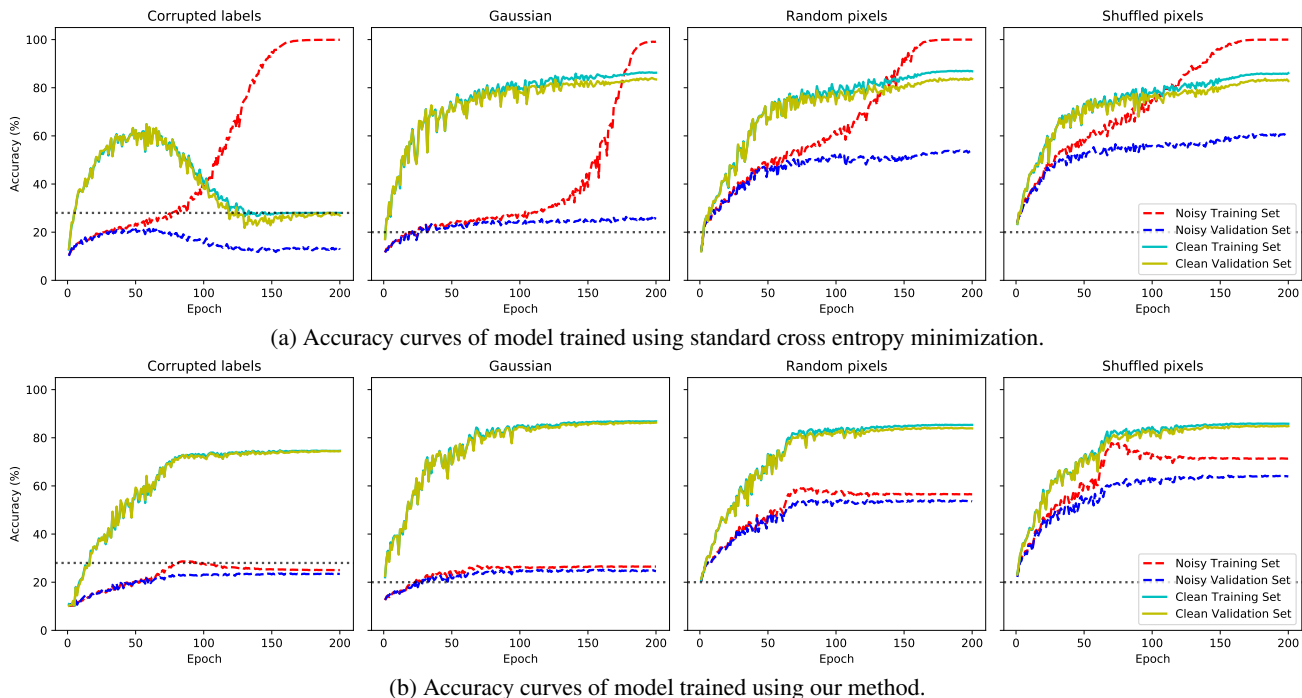


Figure 6: Accuracy curves of model trained on noisy CIFAR10 training set with 80% noise rate. The horizontal dotted line displays the percentage of clean data in the training sets. It shows that our observations in Section 2 hold true even when extreme label noise injected.

## A. Experimental Setups

### A.1. Double descent phenomenon

Following previous work (Nakkiran et al., 2019), we optimize all models using Adam (Kingma & Ba, 2014) optimizer with fixed learning rate of 0.0001, batch size of 128, common data augmentation, weight decay of 0 for 4,000 epochs. For our approach, we use the hyper-parameters  $E_s = 40$ ,  $\alpha = 0.9$  for standard ResNet-18 (width of 64) and dynamically adjust them for other models according to the relation of model capacity  $r = \frac{64}{\text{width}}$  as:

$$E_s = 40 \times r; \quad \alpha = 0.9 \frac{1}{r}. \quad (7)$$

### A.2. Adversarial training

Szegedy et al. (2013) reported that imperceptible small perturbations around input data (i.e., adversarial examples) can cause ERM trained deep neural networks to make arbitrary predictions. Since then, a large literature devoted to improving the adversarial robustness of deep neural networks. Among them, adversarial training algorithm TRADES (Zhang et al., 2019) achieves state-of-the-art performance. TRADES decomposed robust error (w.r.t adversarial examples) to sum of natural error and boundary error, and proposed to minimize:

$$\mathbb{E}_{\mathbf{x}, \mathbf{y}} \left\{ \text{CE}(\mathbf{p}(\mathbf{x}), \mathbf{y}) + \max_{\|\tilde{\mathbf{x}} - \mathbf{x}\|_\infty \leq \epsilon} \text{KL}(\mathbf{p}(\mathbf{x}), \mathbf{p}(\tilde{\mathbf{x}})) / \lambda \right\}, \quad (8)$$

where  $\mathbf{p}(\cdot)$  is the model prediction,  $\epsilon$  is the maximal allowed perturbation, CE stands for cross entropy, KL stands for Kullback-Leibler divergence. The first term corresponds to ERM that maximizes the natural accuracy; the second term pushes the decision boundary away from data points to improve adversarial robustness; the hyper-parameter  $1/\lambda$  controls the trade-off between natural accuracy and adversarial robustness. We evaluate self-adaptive training on this task by replacing the first term of Equation (8) with our approach.

Our experiments are based on the official open-sourced implementation<sup>1</sup> of TRADES (Zhang et al., 2019). Concretely, we

<sup>1</sup><https://github.com/yaodongyu/TRADES>

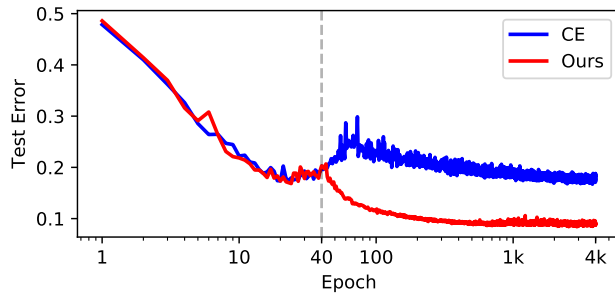


Figure 7: Self-adaptive training vs. ERM on the error-epoch curve. We train the standard ResNet-18 networks (i.e., width of 64) on the CIFAR10 dataset with 15% randomly-corrupted labels and report the test errors on the clean data. The dashed vertical line represents the initial epoch  $E_s$  of our approach. It shows that self-adaptive training has significantly diminished epoch-wise double-descent phenomenon.

conduct experiments on CIFAR10 dataset (Krizhevsky & Hinton, 2009) and use WRN-34-10 (Zagoruyko & Komodakis, 2016) as base classifier. For training, we use initial learning rate of 0.1, batch size of 128, 100 training epochs. The learning rate is decayed at 75-th, 90-th epoch by a factor of 0.1. The adversarial example  $\tilde{x}_i$  is generated dynamically during training by projected gradient descent (PGD) attack (Madry et al., 2017) with maximal  $\ell_\infty$  perturbation  $\epsilon$  of 0.031, perturbation step size of 0.007, number of perturbation steps of 10. The hyper-parameter  $1/\lambda$  of TRADES is set to 6 as suggested by original paper,  $E_s, \alpha$  of our approach is set to 70, 0.9, respectively. For evaluation, we report robust accuracy  $\frac{1}{n} \sum_i \mathbb{1}\{\arg\max p(\tilde{x}_i) = \arg\max y_i\}$ , where adversarial example  $\tilde{x}$  is generated by white box  $\ell_\infty$  untargeted PGD attack with  $\epsilon$  of 0.031, perturbation step size of 0.007, number of perturbation steps of 20.

### A.3. ImageNet

We use ResNet-50/101 (He et al., 2016) as base classifier. Following original paper (He et al., 2016) and (Loshchilov & Hutter, 2016; Goyal et al., 2017), we use SGD to optimize the networks with batch size of 768, base learning rate of 0.3, momentum of 0.9, weight decay of 0.0005 and total training epoch of 95. The learning rate is linearly increased from 0.0003 to 0.3 in first 5 epochs (i.e., warmup), and then decayed using cosine annealing schedule (Loshchilov & Hutter, 2016) to 0. Following common practice, we use random resizing, cropping and flipping augmentation during training. The hyper-parameters  $E_s$  and  $\alpha$  of our approach is set to 50 and 0.99, respectively. The experiments are conducted on PyTorch (Paszke et al., 2019) with distributed training and mixed precision training<sup>2</sup> for acceleration.

### A.4. Selective classification

The experiments are base on official open-sourced implementation<sup>3</sup> of Deep Gamblers to ensure fair comparison. We use the VGG-16 network (Simonyan & Zisserman, 2014) with batch normalization (Ioffe & Szegedy, 2015) and dropout (Srivastava et al., 2014) as base classifier in all experiments. The network is optimized using SGD with initial learning rate of 0.1, momentum of 0.9, weight decay of 0.0005, batch size of 128, total training epoch of 300. The learning rate is decayed by 0.5 in every 25 epochs. For our method, we set the hyper-parameters  $E_s = 0, \alpha = 0.99$ .

## B. Additional Experimental Results

### B.1. Improved generalization

We repeat the same experiments as in Figure 1 of main text by injecting extreme noise (i.e., noise rate of 80%) into CIFAR10 dataset. We report the corresponding accuracy curves in Figure 6, which demonstrates that our observations in Section 2 hold true even when random noise dominates training data.

### B.2. Epoch-wise double descent phenomenon

Nakkiran et al. (2019) reported that, for sufficient large model, test error-training epoch curve also exhibits double-descent phenomenon, which they termed *epoch-wise double descent*. In Figure 7, we reproduce the epoch-wise double descent

<sup>2</sup><https://github.com/NVIDIA/apex>

<sup>3</sup><https://github.com/Z-T-WANG/NIPS2019DeepGamblers>



Table 5: Test Accuracy (%) on CIFAR10 and CIFAR100 datasets with various levels of uniform label noise injected to training set. We show that considerable gains can be obtained when combined with SCE loss.

METHOD	CIFAR10				CIFAR100			
	LABEL NOISE RATE				LABEL NOISE RATE			
	0.2	0.4	0.6	0.8	0.2	0.4	0.6	0.8
SCE (WANG ET AL., 2019)	90.15	86.74	80.80	46.28	71.26	66.41	57.43	26.41
OURS	94.14	92.64	89.23	78.58	75.77	71.38	62.69	38.72
OURS + SCE	<b>94.39</b>	<b>93.29</b>	<b>89.83</b>	<b>79.13</b>	<b>76.57</b>	<b>72.16</b>	<b>64.12</b>	<b>39.61</b>

phenomenon on ERM and inspect self-adaptive training. We observe that our approach (the red curve) exhibits slight double-descent due to overfitting starts before initial  $E_s$  epochs. As the training targets being updated (i.e., after  $E_s = 40$  training epochs), the red curve undergoes monotonous decrease. This observation again indicates that double-descent phenomenon may stem from overfitting of noise and can be avoided by our algorithm.

### B.3. Cooperation with Symmetric Cross Entropy

Wang et al. (2019) showed that Symmetric Cross Entropy (SCE) loss is robust to underlying label noise in training data. Formally, given training target  $t_i$  and model prediction  $p_i$ , SCE loss is defined as:

$$\mathcal{L}_{sce} = -w_1 \sum_j t_{i,j} \log p_{i,j} - w_2 \sum_j p_{i,j} \log t_{i,j}, \tag{9}$$

where the first term is the standard cross entropy loss and the second term is the reversed version. In this section, we show that self-adaptive training can cooperate with this noise-robust loss and enjoy further performance boost without extra cost.

**Setup** The Most experiments settings are kept the same as Section 3.2. For the introduced hyper-parameters  $w_1, w_2$  of SCE loss, we directly set them to 1, 0.1, respectively, in all our experiments.

**Results** We summarize the results in Table 5. We can see that, although self-adaptive training already achieves very strong performance, considerable gains can be obtained when equipped with SCE loss. Concretely, the improvement is as large as 1.5% when label noise of 60% injected to CIFAR100 training set. It also indicates that our approach is flexible and can be further extended.